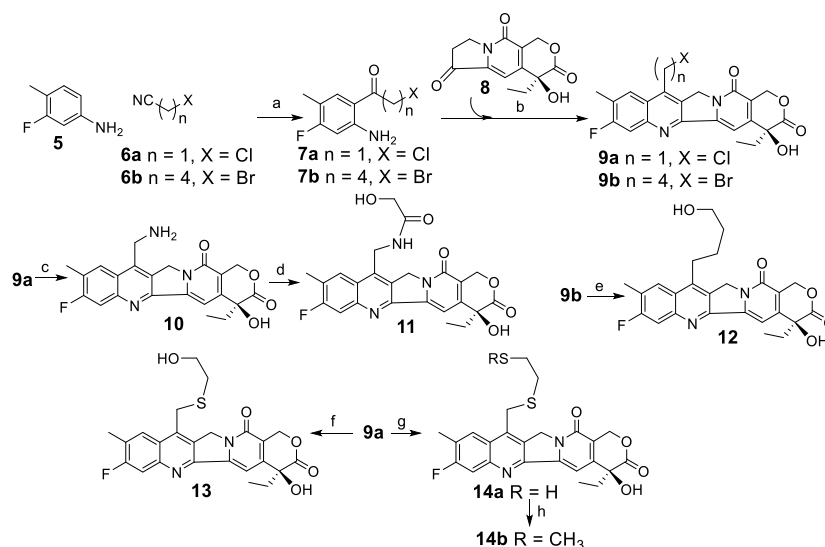


Figure 2. Depiction of DXd-bearing ADCs and processing in cells. DAR stands for drug to antibody ratio.

### Scheme 1. Synthesis of Camptothecin Derivatives<sup>a</sup>



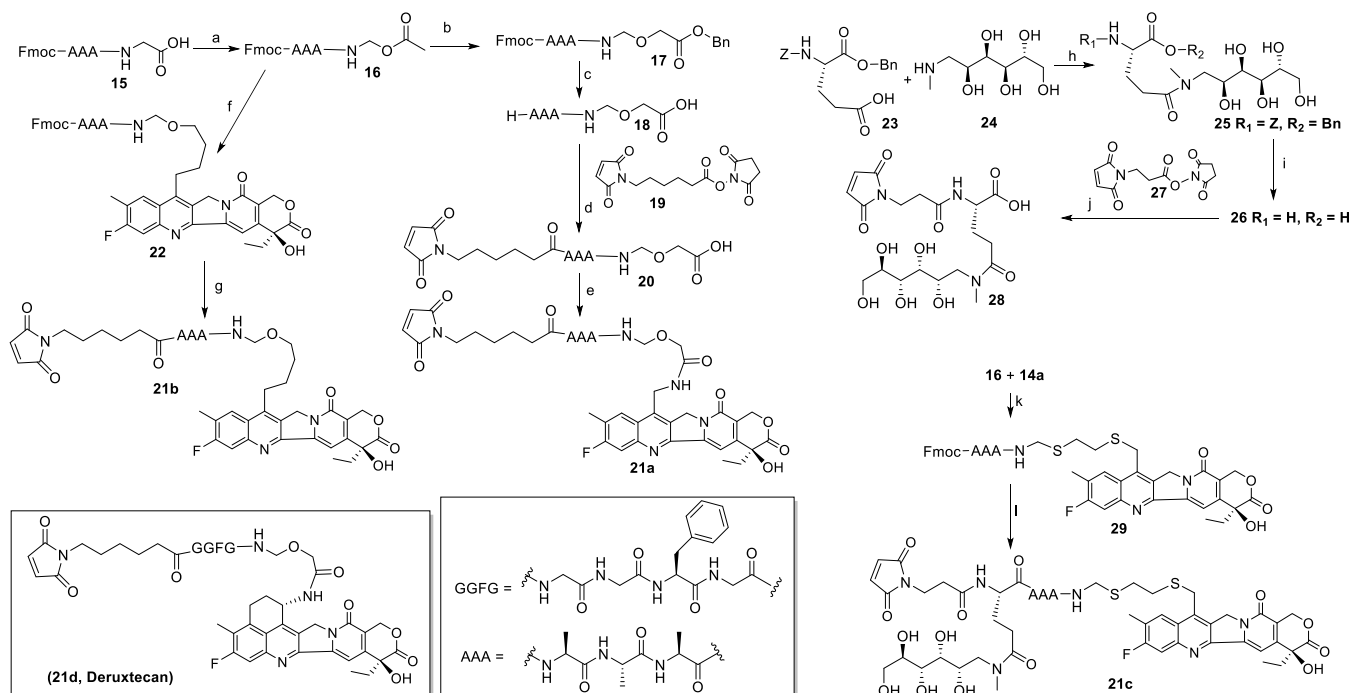
<sup>a</sup>Reagents and conditions: (a) BCl<sub>3</sub>, AlCl<sub>3</sub>, ~39%, (b) PPTS, ~78% (c) NaN<sub>3</sub>; P(OEt)<sub>3</sub>; HCl/H<sub>2</sub>O 57%, (d) glycolic acid DMTMM 93%, (e) HMPA/H<sub>2</sub>O 101 °C, 51%, (f) 2-mercaptoethanol, TEA, 78%, (g) 1,2-dimercaptoethane, DIPEA, 47%, (h) CH<sub>3</sub>I, DIPEA 54%.

the C11 position typically increases cytotoxicity several fold, and the carbon 20 center must be in the *S* configuration for the molecule to maintain activity.<sup>6</sup> Exatecan (**2**) bears an additional F ring and was found to be less prone to hydrolysis in human plasma, with ~30% remaining in the E-ring closed form at equilibrium.<sup>7</sup> The improved lactone stability has been attributed to effects of the C11 fluorine substituent and the F-ring.<sup>8</sup>

A few ADCs that use camptothecin derivatives as the payload are currently in clinical evaluation, and promising data is emerging.<sup>9–12</sup> One such ADC, DS-8201a (**3a**), depicted in Figure 2, binds to human epidermal growth factor receptor 2 (HER2) on targeted cells and is then internalized into catabolic vesicles. Proteases cleave the peptide linker, followed by concomitant amine immolation to release the highly cytotoxic metabolite DXd (**4**), Figure 2. This ADC has shown impressive results in clinical trials, including a 53% overall response rate (ORR) in HER2+ breast cancer patients who no longer respond to the ADC T-DM1,<sup>11</sup> and a 58% ORR in HER2+ nonsmall cell lung cancer.<sup>10</sup> We therefore wished to conduct SAR studies to provide new camptothecin-linker constructs and to determine if ADCs bearing these derivatives would have a similar or improved therapeutic index (TI) in preclinical models.

The F-ring of DXd has a chiral center, which complicates synthetic efforts and SAR studies. Also, two ADCs bearing the less potent camptothecin SN-38, via a linkage that stabilizes the E-ring, or through a linkage that does not, were found to have similar *in vivo* efficacies.<sup>13</sup> This calls into question if the F-ring of DXd, which potentially stabilizes the E-ring, is required. We

therefore investigated if an F-ring was beneficial for camptothecin-ADCs. Another important aspect of ADC design is its ability to induce bystander killing, an effect where ADCs not only kill targeted antigen positive (Ag+) cells but also some of the nearby (bystander) cells in a tumor, which may be Ag+ or antigen negative (Ag-). There is mounting evidence that ADCs with this capability are more efficacious in tumor xenograft models.<sup>14–17</sup> For bystander killing to occur, ADC metabolites must be membrane permeable in order to diffuse into proximal nontargeted cells. Compounds typically become more membrane permeable as their hydrophobicity increases.<sup>18</sup> Consequently, if other attributes are not affected, an ADC's bystander killing should be enhanced by increasing the hydrophobicity of its metabolite(s). We therefore synthesized payloads with different hydrophobicities to determine if ADCs using them would induce varying degrees of bystander killing. Lastly, although it is not dose limiting in the clinic, DXd bearing ADCs have significant gastrointestinal (GI) toxicity,<sup>10,11,19</sup> and DXd itself is not metabolized by liver.<sup>20</sup> Liver inactivation of camptothecin-ADC metabolites could potentially reduce GI toxicity. Compounds containing sulfide moieties are typically easily oxidized<sup>21</sup> and can often be inactivated in liver.<sup>22,23</sup> Also, thiol-bearing compounds can be *S*-methylated by cells, facilitating inactivation through oxidation to sulfoxides and sulfones in the liver.<sup>22,23</sup> We therefore designed ADCs that could efficiently release camptothecin metabolites that contain a sulfide or thiol moiety. All synthetic and analytical procedures

Scheme 2. Synthesis of Camptothecin Payloads<sup>a</sup>

<sup>a</sup>Reagents and conditions: (a)  $\text{Pb}(\text{OAc})_4$ , AcOH,  $\text{Cu}(\text{OAc})_2$  62%, (b)  $\text{HOCH}_2\text{COOBn}$ , 20% TFA in  $\text{CH}_2\text{Cl}_2$ , 59%, (c) 15% morpholine in DMF; 10% Pd-C/ $\text{H}_2$  20 PSI, 69%, (d) DMF, DIPEA 63%, (e) **10**, DMTMM, TEA, 36%, (f) **12**, 4% HCl in DMF, 48%, (g) 15% morpholine in DMF; **19**, DIPEA, 42%, (h) DMTMM 68%, (i) 10% Pd-C/ $\text{H}_2$  20 PSI, 94%, (j) DIPEA 55%, (k) 20% TFA in  $\text{CH}_2\text{Cl}_2$ , 56%, (l) 15% morpholine in DMF; **28**, TEA, DMTMM, 24%.

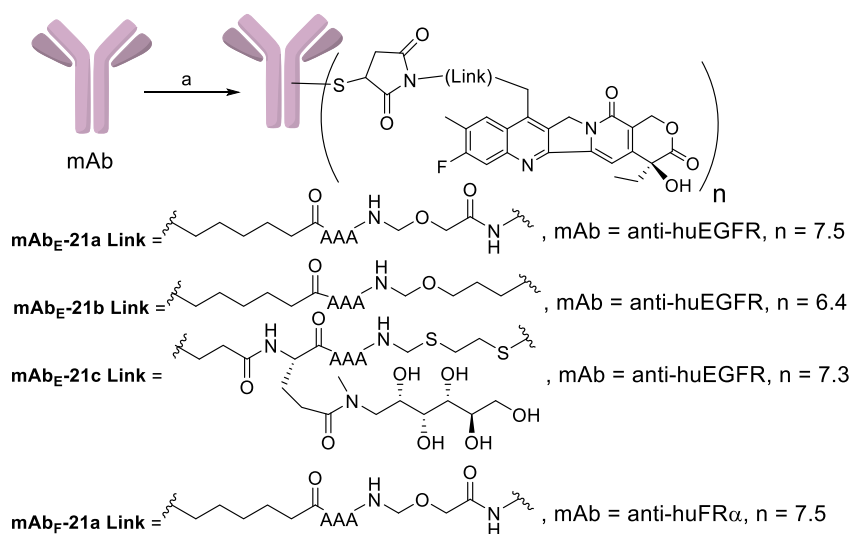


**Figure 3.** Preparation of **mAb-21a–mAb-21c**. Reagents and conditions (a) TCEP, one of **21a–21c**, SEC. Conjugations with **21d** were performed identically using an anti-huEGFR, anti-huFR $\alpha$ , or anti-chKTI mAb. The value  $n$  indicates the drug per antibody ratio (DAR).

are detailed in the supplementary section and briefly described herein.

A set of camptothecin derivatives was prepared as depicted in Scheme 1. The aniline **5** was acylated with chloroacetonitrile (**6a**) or 5-bromopentyl nitrile (**6b**) in the presence of Lewis acids,  $\text{BCl}_3$  and  $\text{AlCl}_3$ , to give **7a** or **7b**, respectively. Each compound was then reacted with commercially available **8** in the presence of a catalytic amount of pyridinium *p*-toluene sulfonate (PPTS) to give **9a** or **9b**, respectively.<sup>24</sup> Compound **9a** was reacted with sodium azide, then reduced to give **10**, which was coupled to glycolic acid giving **11**. Reaction of **9b** with 15%

water in HMPA at 101 °C overnight gave **12**. The chlorine atom of **9a** was displaced with 2-mercaptoethanol or 1,2-dimercaptoethane in *N,N*-dimethylformamide (DMF) and *N,N*-diisopropylethylamine (DIPEA) to give **13** or **14a**, respectively. Methylation of **14a** with iodomethane gave **14b**.

Camptothecin payloads, capable of being conjugated to a mAb, were synthesized as shown in Scheme 2. The protected peptide (**15**, Fmoc-Ala-Ala-Ala-Gly-OH) was prepared by solid phase synthesis using standard procedures.<sup>25</sup> Oxidative decarboxylation of **15** using lead tetraacetate gave **16**,<sup>26</sup> which was then reacted with the benzyl ester of glycolic acid in a

solution of 20% trifluoroacetic acid (TFA) in dichloromethane to give **17**. Deprotection of **17** with morpholine, followed by hydrogenation with 10% palladium on carbon gave **18**, which was then reacted with the heterobifunctional reagent **19** to give **20**. Coupling of **20** with compound **10** using (4-(4,6-dimethoxy-1,3,5-triazin-2-yl)-4-methyl-morpholinium chloride) (DMTMM) gave payload **21a**. Displacement of the acetate moiety of **16** with **12** in DMF containing 4% HCl gave **22**, which was then deprotected with morpholine and reacted with **19** to give **21b**. Compound **19** has five methylene units, making it and the payloads that incorporate it fairly hydrophobic. ADCs that are highly hydrophobic can form aggregates and are potentially cleared from circulation *in vivo* faster than more hydrophilic conjugates.<sup>27</sup> Adding a polar moiety to the linker was therefore desired, but preferably at a location that would not affect the hydrophobicity of an ADC's released metabolite. Consequently, a more hydrophilic derivative, bearing a polyhydroxyl moiety and a maleimide, to enable conjugation was prepared. Z-L-Glutamic acid benzyl ester **23** was coupled to *N*-methyl-D-glucamine (**24**) using DMTMM to give **25**, which was deprotected by hydrogenation in methanol/water to **26**. The heterobifunctional linker **27** was then coupled to **26** to give **28**. To prepare a sulfide-bearing payload, **16** was reacted with **14a** in dilute acid to give **29**. Deprotection of **29** with morpholine, followed by coupling to **28** using DMTMM gave **21c**.

Exatecan mesylate was purchased from Abzena and used to prepare the F-ring bearing camptothecins **DXd** (**4**) and the linkable payload deruxetecan (**21d**) as described by Agatsuma et al.<sup>28</sup> The conjugates **mAb<sub>E</sub>-21d**, **mAb<sub>F</sub>-21d**, and **mAb<sub>ctrl</sub>-21d** depicted in Figure 2 and ADCs bearing new payloads were prepared as shown schematically in Figure 3.<sup>28</sup> The humanized anti-huEGFR and anti-huFR $\alpha$  antibodies, which bind to human epidermal growth factor receptor 1 (EGFR) or to human folate receptor-alpha (FR $\alpha$ ), respectively, were used to prepare ADCs capable of targeting EGFR+ or FR $\alpha$ + cells. The four interchain disulfide bonds of each mAb were reduced with tris(2-carboxyethyl)phosphine (TCEP). The eight free cysteine thiols of the mAb were then reacted with one of the payloads (**21a**–**21d**), and side products were removed by size exclusion chromatography (SEC). The anti-chKTI antibody, a chimeric antibody targeting Kunitz soybean trypsin inhibitor, was also conjugated to **21d** to give a control ADC (**ADC<sub>ctrl</sub>**), which does not bind to mouse or human cells. The drug to antibody ratio (DAR) for each ADC is shown in Figure 2 and Scheme 2. Similar to the published conjugation procedure, full 8.0 DAR ADCs were not obtained presumably because some free thiols reformed interchain disulfide bonds.

The ADCs (**mAb<sub>E</sub>-21a**–**mAb<sub>E</sub>-21d**) were assayed for cytotoxicity and bystander killing, Table 1. As expected, they were highly potent against targeted Ag+ cells and much less potent against the cells in the presence of unconjugated antibodies that block binding of the conjugate, or toward nontargeted Ag– cells. In the bystander killing assay, several concentrations of a conjugate were incubated with a coculture of Ag+ cells and Ag–/*luc* cells, (Ag– cells transfected with luciferase gene) in U-bottom 96-well plates. The ADC is taken up by Ag+ cells, then metabolites are released inside the cell and kill it, and potentially diffuse into and kill the Ag– cells. Survival of Ag–/*luc* cells was measured with an assay that detects only luciferase-positive cells. ADCs **mAb<sub>E</sub>-21b** and **mAb<sub>E</sub>-21c** induced the highest level of bystander killing even though they were slightly less cytotoxic to Ag+ cells (Table 1). The metabolites from these conjugates have not yet been identified.

**Table 1. In Vitro Cytotoxicity and Bystander Killing Activity of ADCs **mAb<sub>E</sub>-21a**–**mAb<sub>E</sub>-21d****

ADC	cell lines IC <sub>50</sub> (M)		bystander IC <sub>50</sub> (M) <sup>c</sup>
	NL <sup>a</sup> Ag–	Mb <sup>b</sup> Ag+	Ag–:Ag+
<b>mAb<sub>E</sub>-21a</b>	1 × 10 <sup>−7</sup>	4 × 10 <sup>−10</sup>	4 × 10 <sup>−9</sup>
<b>mAb<sub>E</sub>-21b</b>	5 × 10 <sup>−7</sup>	7 × 10 <sup>−10</sup>	5 × 10 <sup>−10</sup>
<b>mAb<sub>E</sub>-21c</b>	6 × 10 <sup>−7</sup>	1 × 10 <sup>−9</sup>	6 × 10 <sup>−10</sup>
<b>mAb<sub>E</sub>-21d</b>	1 × 10 <sup>−7</sup>	7 × 10 <sup>−10</sup>	2 × 10 <sup>−9</sup>

<sup>a</sup>Namalwa/*luc* cells (NL). <sup>b</sup>MDA-MB-468 cells (Mb). <sup>c</sup>Bystander killing indicates the IC<sub>50</sub> for killing Ag– cells in the mixture of Ag– and Ag+ cells (Ag–:Ag+). The Ag– and Ag+ cells are NL and Mb, respectively.

However, if these new conjugates are metabolized by cells, similarly to ADC **3a**, then **mAb<sub>E</sub>-21a**, **mAb<sub>E</sub>-21b**, **mAb<sub>E</sub>-21c**, and **mAb<sub>E</sub>-21d** should predominantly give metabolites **11**, **12**, **14a**, and **4** (**DXd**), respectively. Also, **14a** could potentially be *S*-methylated in cells to give **14b**. Compounds **12**, **14a**, and **14b**, lacking a polar amide in their C7 side chains, are expected to be more hydrophobic than **11** or **DXd**. We postulate that the metabolites from each ADC will have similar cytotoxicities when produced inside cells, but those that are more hydrophobic diffuse more efficiently into Ag– cells.

Thiol-bearing compounds, such as **14a**, can react with cysteine or other charged disulfide containing molecules in cell culture, to become poorly membrane permeable.<sup>23</sup> Therefore, only the *in vitro* cytotoxicities of **11**, **12**, **13**, **14b**, and **DXd** were determined, Table 2. The more hydrophobic compounds **12**, **13**, and **14b**

**Table 2. In Vitro Cytotoxicities of Unconjugated Compounds against HSC-2 and Namalwa/*luc* (NL) Cells**

compound	cell line IC <sub>50</sub> , M	
	HSC-2	NL <sup>a</sup>
<b>DXd</b> ( <b>4</b> )	1 × 10 <sup>−9</sup>	6 × 10 <sup>−10</sup>
<b>11</b>	2 × 10 <sup>−9</sup>	9 × 10 <sup>−10</sup>
<b>12</b>	5 × 10 <sup>−10</sup>	2 × 10 <sup>−10</sup>
<b>13</b>	4 × 10 <sup>−10</sup>	2 × 10 <sup>−10</sup>
<b>14b</b>	6 × 10 <sup>−10</sup>	2 × 10 <sup>−10</sup>

<sup>a</sup>Namalwa/*luc* cells (NL).

had higher potencies than **11** and **DXd** against the two cell lines tested. Further studies will be needed to determine how efficiently metabolites are released from ADCs **mAb-21a**–**mAb-21d**, and if the postulated metabolites are indeed formed.

The antitumor activity of **mAb<sub>E</sub>-21a** and **mAb<sub>E</sub>-21d** was evaluated in nude mice bearing human head and neck squamous cell carcinoma EGFR-positive HSC-2 xenografts, Figure 4 (top), which display a high level of antigen expression (H score of 270), as determined using immunohistochemical methods as previously described.<sup>29</sup> The activities of **mAb<sub>E</sub>-21a**, **mAb<sub>E</sub>-21b**, and **mAb<sub>E</sub>-21d** were also evaluated in nude mice bearing nonsmall cell lung cancer (NSCLC) squamous cell H1703 xenografts, wherein the antigen expression was lower (H score of 125) Figure 4 (bottom). Groups of six mice per test article were dosed as described in the figures. Control groups were dosed with vehicle or the nontargeted conjugate **ADC<sub>ctrl</sub>**. Data from these studies was interpreted using standardized methods.<sup>30</sup> Tables containing T/C, PRs, and CRs for each study are shown in the Supporting Information. In both models, little efficacy was seen for the nontargeted **ADC<sub>ctrl</sub>** group, demonstrating targeting specificity. **mAb<sub>E</sub>-21a** and **mAb<sub>E</sub>-21d** showed similar

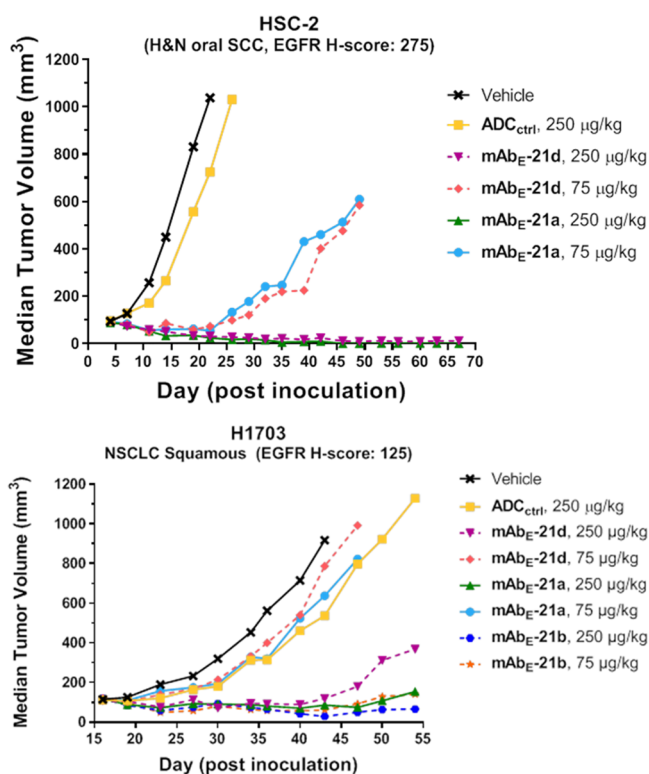


**Figure 4.** Antitumor activity of vehicle, ADC<sub>ctrl</sub>, mAb<sub>E</sub>-21a, and mAb<sub>E</sub>-21d at 75 and 250 μg/kg in HSC-2 (top); and vehicle, ADC<sub>ctrl</sub>, mAb<sub>E</sub>-21a, mAb<sub>E</sub>-21b, and mAb<sub>E</sub>-21c at 75 and 250 μg/kg in H1703 (bottom) mouse xenograft models. Dosing based on payload (75 and 250 μg/kg are ~3 and ~10 mg/kg based on antibody).

dose-dependent antitumor activity in both the HSC-2 and H1703 EGFR+ xenograft models. The T/C and number of PRs and CRs were not significantly different between the mAb<sub>E</sub>-21a and mAb<sub>E</sub>-21d groups in either model, see Supporting Information. mAb<sub>E</sub>-21b was only tested in the lower antigen expressing H1703 model and was found to be significantly more active than the other two ADCs tested. Thus, at a dose of 75 μg/kg it had comparable activity, including T/C, PRs, and CRs, to that obtained with a higher dose (250 μg/kg) of the mAb<sub>E</sub>-21a and mAb<sub>E</sub>-21d groups. Also, no significant body weight loss was observed for mice in any group, indicating that the conjugates were well tolerated (data not shown).

A pharmacokinetic study was conducted in mice to determine the stability and clearance rates of ADCs mAb<sub>E</sub>-21a and mAb<sub>E</sub>-21d. Groups of mice (3 mice/group) were dosed with the two ADCs at 10 mg/kg to determine the averaged clearance of their antibody components and retained bioactivity over time. Blood samples were taken at 2 min, 1 day, and 3 days post-inoculation and assayed for total anti-huEGFR mAb (μg/mL), which was determined by a sandwich enzyme-linked immunosorbent assay (ELISA), as previously described.<sup>31</sup> The clearance of the antibody component was found to be similar for both conjugates (Figure 5). Retained bioactivity of the ADC in the plasma samples over time was determined in cytotoxicity assays with Ag+ or Ag- cells. The ADCs retained most of their activity against Ag+ cells at each of the time points while remaining over 200-fold less active against Ag- cells, indicating that the cytotoxicities were due to intact ADC, with little or no contribution from any released payload (Figures 5 and 6).

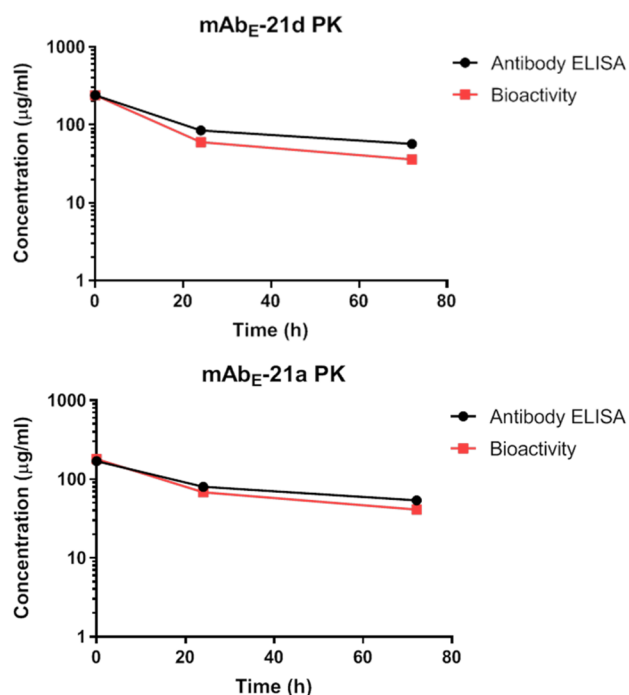


**Figure 5.** Plots of concentration (μg/mL) vs time of the mAb component (average) and retained bioactivity (pooled samples) of ADCs at 2 min, 1 day, and 3 day time points post administration in mice: mAb<sub>E</sub>-21d (top) and mAb<sub>E</sub>-21a (bottom).

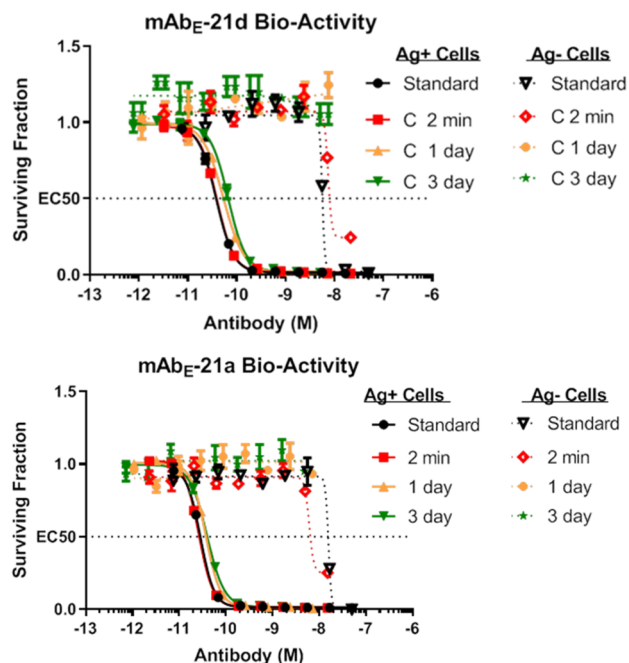


**Figure 6.** In vitro cytotoxicities of ADCs against Ag+ and Ag- cells. ADC standard in formulation (standard) or blood serum (pooled) containing ADC taken at 2 min, 1 day, or 3 days post administration into mice for mAb<sub>E</sub>-21d (top) or mAb<sub>E</sub>-21a (bottom).

The tolerability of the ADCs was then assessed in mice. Groups of mice (3/group) were administered a single intravenous dose of vehicle control, mAb<sub>E</sub>-21a, or mAb<sub>E</sub>-21d at 5000 μg/kg based on payload (~200 mg/kg based on Ab), Figure 7. Both conjugates were well tolerated. The maximum tolerated dose (MTD), as defined by body weight loss of 20% or

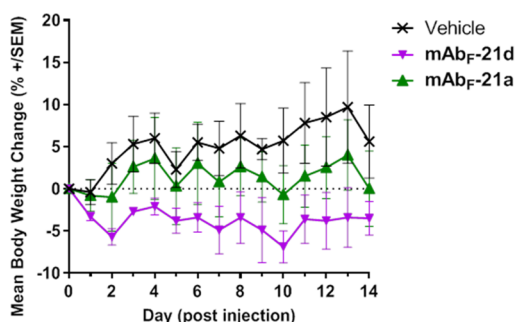


**Figure 7.** Mouse tolerability of noncross-reactive ADCs at 5000  $\mu\text{g}/\text{kg}$  payload dose ( $\sim 200$  mg/kg based on the Ab component).

more, was not reached for either ADC group 14 days post injection. However, the mice treated with **mAb<sub>F</sub>-21d** lost significantly more body weight than those treated with vehicle or **mAb<sub>F</sub>-21a** in these initial studies.

In conclusion, camptothecins that do not have an F-ring are highly promising ADC payloads, which are easily derivatized on their A and B rings. This allows simplified preparation of camptothecin ADCs for SAR studies. The TI of conjugates that use payload **21a** appears to be comparable to those containing the F-ring bearing payload **21d**. An initial study indicated that an ADC with **21b** was  $\sim 3$ -fold more efficacious than ADCs bearing the **21a** or **21d** payloads. Additional studies will be needed to evaluate these ADCs, such as identification of the structures and formation efficiencies of their metabolites and comparisons of their pharmacokinetics and tolerabilities. We have previously used the concept of increasing metabolite hydrophobicity to increase the bystander killing of conjugates bearing maytansinoids and believe this strategy will be generally applicable to ADCs bearing other payloads.<sup>32,33</sup>

## ■ ASSOCIATED CONTENT

### 📄 Supporting Information

The Supporting Information is available free of charge on the ACS Publications website at DOI: 10.1021/acsmchemlett.9b00301.

Detailed experimental procedures (PDF)

## ■ AUTHOR INFORMATION

### Corresponding Author

\*E-mail: waynecwiddison@gmail.com.

### ORCID

Wayne C. Widdison: 0000-0003-2463-1440

### Author Contributions

The manuscript was written through contributions of all authors. All authors have given approval to the final version of the manuscript.

### Funding

This study was supported by ImmunoGen, Inc.

### Notes

The authors declare no competing financial interest.

## ■ ACKNOWLEDGMENTS

We would like to thank Richard Gregory and Joseph Kenny for their valuable suggestions.

## ■ ABBREVIATIONS

ADC, antibody–drug conjugate; Bn, benzyl; DAR, drug per antibody ratio; DIPEA, *N,N*-diisopropylethylamine; DMF, *N,N*-dimethylformamide; DCM, dichloromethane; DMSO, dimethyl sulfoxide; DMTMM, (4-(4,6-dimethoxy-1,3,5-triazin-2-yl)-4-methyl-morpholinium chloride); Fmoc, 9-fluorenylmethoxycarbonyl; HMPA, hexamethyl phosphoramide; NHS, *N*-hydroxysuccinimide ester; NMM, *N*-methyl morpholine; PPTS, pyridinium *p*-toluene sulfonate; TCEP, tris(2-carboxyethyl)-phosphine; TEA, triethylamine; TFA, trifluoroacetic acid; SEC, size-exclusion chromatography; Z, benzyloxycarbonyl

## ■ REFERENCES

- (1) Chari, R. V.; Miller, M. L.; Widdison, W. C. Antibody-drug conjugates: An emerging concept in cancer therapy. *Angew. Chem., Int. Ed.* **2014**, *53*, 3796–3827.
- (2) Donaghy, H. Effects of antibody, drug and linker on the preclinical and clinical toxicities of antibody-drug conjugates. *MAbs* **2016**, *8*, 659–71.
- (3) Sedlacek, H. H.; Steinstraesser, A.; Kuhlmann, L.; Schwarz, A.; Seidel, L.; Seemann, G.; Kraemer, H.-P.; Bosslet, K. Monoclonal antibodies in tumor therapy. *Contributions in Oncology*, Eckhardt, S., Holzner, J. H., Nagel, G. A., Eds.; Karger: Munchen, 1988; Vol. 32, pp 81–100.
- (4) Hsiang, Y. H.; Hertzberg, R.; Hecht, S.; Liu, L. F. Camptothecin induces protein-linked DNA breaks via mammalian DNA topoisomerase I. *J. Biol. Chem.* **1985**, *260*, 14873–8.
- (5) Burke, T. G.; Mi, Z. Preferential binding of the carboxylate form of camptothecin by human serum albumin. *Anal. Biochem.* **1993**, *212*, 285–7.
- (6) Yaegashi, T.; Sawada, S.; Nagata, H.; Furuta, T.; Yokokura, T.; Miyasaka, T. Synthesis and antitumor activity of 20(S)-camptothecin derivatives. A-ring-substituted 7-ethylcamptothecins and their E-ring-modified water-soluble derivatives. *Chem. Pharm. Bull.* **1994**, *42*, 2518–25.
- (7) Minami, H.; Fujii, H.; Igarashi, T.; Itoh, K.; Tamanoi, K.; Oguma, T.; Sasaki, Y. Phase I and pharmacological study of a new camptothecin derivative, exatecan mesylate (DX-8951f), infused over 30 minutes every three weeks. *Clin. Cancer Res.* **2001**, *7*, 3056–64.
- (8) Venditto, V. J.; Simanek, E. E. Cancer therapies utilizing the camptothecins: a review of the in vivo literature. *Mol. Pharmaceutics* **2010**, *7*, 307–49.
- (9) Bardia, A.; Mayer, I. A.; Diamond, J. R.; Moroosse, R. L.; Isakoff, S. J.; Starodub, A. N.; Shah, N. C.; O'Shaughnessy, J.; Kalinsky, K.; Guarino, M.; Abramson, V.; Juric, D.; Tolaney, S. M.; Berlin, J.; Messersmith, W. A.; Ocean, A. J.; Wegener, W. A.; Maliakal, P.; Sharkey, R. M.; Govindan, S. V.; Goldenberg, D. M.; Vahdat, L. T. Efficacy and safety of anti-Trop-2 antibody drug conjugate sacituzumab govitecan (IMMU-132) in heavily pretreated patients with metastatic triple-negative breast cancer. *J. Clin. Oncol.* **2017**, *35*, 2141–2148.
- (10) Planchard, D.; Li, B. T.; Murakami, H.; Shiga, R.; Lee, C. C.; Wang, K.; Jänne, P. A. 183TiPa phase II study of [fam-] trastuzumab deruxtecan (DS-8201a) in HER2-overexpressing or mutated advanced non-small cell lung cancer. *Ann. Oncol.* **2019**, *30*, mdz063.081.
- (11) Tamura, K.; Modi, S.; Tsurutani, J.; Takahashi, S.; Krop, I.; Iwata, H.; Wada, R.; Yin, O.; Garimella, T.; Sugihara, M.; Zhang, L.; Lee, C.; Yver, A.; Baselga, J. Abstract P6–17–10: Dose justification for DS-8201a, a HER2-targeted antibody-drug conjugate, for HER2-positive breast cancer: Observed clinical data and exposure-response analyses. *Cancer Res.* **2019**, *79*, P6-17-10.
- (12) Doi, T.; Shitara, K.; Naito, Y.; Shimomura, A.; Fujiwara, Y.; Yonemori, K.; Shimizu, C.; Shimoi, T.; Kuboki, Y.; Matsubara, N.; Kitano, A.; Jikoh, T.; Lee, C.; Fujisaki, Y.; Ogitani, Y.; Yver, A.; Tamura, K. Safety, pharmacokinetics, and antitumor activity of trastuzumab deruxtecan (DS-8201), a HER2-targeting antibody-drug conjugate, in patients with advanced breast and gastric or gastro-oesophageal

tumours: a phase 1 dose-escalation study. *Lancet Oncol.* **2017**, *18*, 1512–1522.

(13) Lau, U. Y.; Benoit, L. T.; Stevens, N. S.; Emmerton, K. K.; Zaval, M.; Cochran, J. H.; Senter, P. D. Lactone stabilization is not a necessary feature for antibody conjugates of camptothecins. *Mol. Pharmaceutics* **2018**, *15*, 4063–4072.

(14) Ogitani, Y.; Hagihara, K.; Oitate, M.; Naito, H.; Agatsuma, T. Bystander killing effect of DS-8201a, a novel anti-human epidermal growth factor receptor 2 antibody-drug conjugate, in tumors with human epidermal growth factor receptor 2 heterogeneity. *Cancer Sci.* **2016**, *107*, 1039–46.

(15) Widdison, W. C.; Ponte, J. F.; Coccia, J. A.; Lanieri, L.; Setiady, Y.; Dong, L.; Skaletskaya, A.; Hong, E. E.; Wu, R.; Qiu, Q.; Singh, R.; Salomon, P.; Fishkin, N.; Harris, L.; Maloney, E. K.; Kovtun, Y.; Veale, K.; Wilhelm, S. D.; Audette, C. A.; Costoplus, J. A.; Chari, R. V. Development of anilino-maytansinoid ADCs that efficiently release cytotoxic metabolites in cancer cells and induce high levels of bystander killing. *Bioconjugate Chem.* **2015**, *26*, 2261–78.

(16) Vasalou, C.; Helmlinger, G.; Gomes, B. A mechanistic tumor penetration model to guide antibody drug conjugate design. *PLoS One* **2015**, *10*, No. e0118977.

(17) Kovtun, Y. V.; Audette, C. A.; Mayo, M. F.; Jones, G. E.; Doherty, H.; Maloney, E. K.; Erickson, H. K.; Sun, X.; Wilhelm, S.; Ab, O.; Lai, K. C.; Widdison, W. C.; Kellogg, B.; Johnson, H.; Pinkas, J.; Lutz, R. J.; Singh, R.; Goldmacher, V. S.; Chari, R. V. Antibody-maytansinoid conjugates designed to bypass multidrug resistance. *Cancer Res.* **2010**, *70*, 2528–37.

(18) Bennion, B. J.; Be, N. A.; McNerney, M. W.; Lao, V.; Carlson, E. M.; Valdez, C. A.; Malfatti, M. A.; Enright, H. A.; Nguyen, T. H.; Lightstone, F. C.; Carpenter, T. S. Predicting a drug's membrane permeability: A computational model validated with in vitro permeability assay data. *J. Phys. Chem. B* **2017**, *121*, 5228–5237.

(19) Nakada, T.; Sugihara, K.; Jikoh, T.; Abe, Y.; Agatsuma, T. The latest research and development into the antibody-drug conjugate, [fam-] trastuzumab deruxtecan (DS-8201a), for HER2 cancer therapy. *Chem. Pharm. Bull.* **2019**, *67*, 173–185.

(20) Nagai, Y.; Oitate, M.; Shiozawa, H.; Ando, O. Comprehensive preclinical pharmacokinetic evaluations of trastuzumab deruxtecan (DS-8201a), a HER2-targeting antibody-drug conjugate, in cynomolgus monkeys. *Xenobiotica* **2019**, *49*, 1086.

(21) Barnard, D.; Bateman, L.; Cunneen, J. I. Oxidation of organic sulfides. In *Organic Sulfur Compounds*, Kharasch, N., Ed.; Pergamon Press: New York, 1961; Vol. 1.

(22) Sun, X.; Widdison, W.; Mayo, M.; Wilhelm, S.; Leece, B.; Chari, R.; Singh, R.; Erickson, H. Design of antibody-maytansinoid conjugates allows for efficient detoxification via liver metabolism. *Bioconjugate Chem.* **2011**, *22*, 728–35.

(23) Widdison, W. C.; Wilhelm, S.; Veale, K.; Costoplus, J.; Jones, G.; Audette, C.; Leece, B.; Bartle, L.; Kovtun, Y.; Chari, R. J. Metabolites of antibody-maytansinoid conjugates: characteristics and *in vitro* potencies. *Mol. Pharmaceutics* **2015**, *12*, 1762–73.

(24) Ejima, A.; Terasawa, H.; Sugimori, M.; Tagawa, H. Antitumor agents. I. Asymmetric synthesis of (S)-camptothecin. *Tetrahedron Lett.* **1989**, *30*, 2639–2640.

(25) Benoiton, N. L. *Chemistry of Peptide Synthesis*; CRC Press, 2006.

(26) Needles, H. L.; Ivanetich, K. Decarboxylation of *N*-acetylaminic acids with lead tetra-acetate in *N,N*-dimethylformamide. *Chem. Ind.* **1967**, *14*, 581.

(27) Lyon, R. P.; Bovee, T. D.; Doronina, S. O.; Burke, P. J.; Hunter, J. H.; Neff-LaFord, H. D.; Jonas, M.; Anderson, M. E.; Setter, J. R.; Senter, P. D. Reducing hydrophobicity of homogeneous antibody-drug conjugates improves pharmacokinetics and therapeutic index. *Nat. Biotechnol.* **2015**, *33*, 733–5.

(28) Agatsuma, T.; Takahashi, S.; Hasegawa, J.; Okajima, D.; Hamada, H.; Yamagushi, M. Anti-trop2 antibody-drug. US Patent 2016/0297890 A1, October 13, 2016.

(29) Detre, S.; Saclani Jotti, G.; Dowsett, M. A "quickscore" method for immunohistochemical semiquantitation: validation for oestrogen receptor in breast carcinomas. *J. Clin. Pathol.* **1995**, *48*, 876–8.

(30) Bissery, M. C.; Guenard, D.; Gueritte-Voegelein, F.; Lavelle, F. Experimental antitumor activity of taxotere (RP 56976, NSC 628503), a taxol analogue. *Cancer Res.* **1991**, *51*, 4845–52.

(31) Xie, H.; Audette, C.; Hoffee, M.; Lambert, J. M.; Blattler, W. A. Pharmacokinetics and biodistribution of the antitumor immunoconjugate, cantuzumab mertansine (huC242-DM1), and its two components in mice. *J. Pharmacol. Exp. Ther.* **2004**, *308*, 1073–82.

(32) Widdison, W. C.; Costoplus, J. A.; Ponte, J. F.; Lanieri, L.; Setiady, Y.; Dong, L.; Skaletskaya, A.; Wu, R.; Qiu, Q.; Kovtun, Y.; Chari, R. V. Peptide-cleavable maytansinoid (ADCs) induce high bystander killing leading to improved anti-tumor activity in vivo. *Cancer Res.* **2017**, *77* (13 Suppl), 2186.

(33) Manuscript submitted for publication.